ELSEVIER

Review

Catalytic significance of organometallic compounds immobilized on mesoporous silica: economically and environmentally important examples

John Meurig Thomas [a,b,*], Robert Raja [c,*]

[a] _Department of Materials Science, University of Cambridge, Pembroke Street, Cambridge CB2 3QZ, UK_
[b] _Davy Faraday Research Laboratory, The Royal Institution of Great Britain, 21 Albemarle Street, London W1S 4BS, UK_
[c] _Department of Chemistry, University of Cambridge, Lensfield Road, Cambridge CB2 1EW, UK_

We dedicate this article to the memory of Professor Colin Eaborn, FRS, a fine chemist and a gentleman

Abstract

Because of the availability of well-defined nanoporous silicas, possessing (controllable) pore diameters of 30 Å to ca. 500 Å, bulky organometallic species may be readily introduced on to the inner walls of these thermally stable, solid supports. Four kinds of highly active catalysts that may be derived from the combination of these two materials are illustrated. First, starting from titanocene dichloride, single-site Ti^{IV}-centered epoxidation catalysts of exceptional activity may be formed. These are now used in the preparation of epoxy polymers and other products from naturally occurring methyl esters of fatty acids, a novel example of sustainable development. Second, asymmetric organometallic species that exhibit good enantioselectivity as homogeneous catalysts (in the hydrogenation of keto-esters, for example) may be significantly improved in their catalytic performance when they are anchored to a concave silica surface, their ee values are boosted by the spatial restrictions imposed by the mesopores within which they are anchored. Examples of three distinct diamino-complexes of Rh(I) are illustrated for the selective hydrogenations of methylbenzoylformate and _E_-α-phenylcinnamic acid. In the third kind of catalyst immobilized on nanoporous silica, several mixed-metal carbonylates are used as precursors. They are firmly anchored to the inner walls and may, by gentle calcining, be converted to bimetallic catalysts [e.g., Ru_6Pd_6, Ru_5Pt and $Ru_{10}Pt_2$] that exhibit very high activity, under mild conditions, in the single-step, solvent-free hydrogenation of a range of economically important unsaturated compounds. The fourth category of immobilized, organometallics illustrated here is of the "ship-in-bottle" kind, where, typically, a chlorinated copperphthalocyanine incarcerated within the cages of zeolite-X efficiently converts methane to methanol and also smoothly oxyhalogenates a range of aromatic compounds (e.g., benzene, phenol, toluene, aniline, anisole and resorcinol) in air, again under mild conditions. The unconventional techniques, both in situ and ex situ, required to characterize all these immobilized catalysts are outlined.
© 2004 Elsevier B.V. All rights reserved.

Keywords: Nanoporous; Organometallic; Immobilized; Single-site; Asymmetric catalysis; Zeozymes; Bimetallic; Solvent-free processes

1. Introduction

There are three main reasons why one would wish to immobilize on to high-area, solid supports organometallic species that are of catalytic significance. First,

* Corresponding authors. Tel.: +441223336335; fax: +441223336017.

E-mail addresses: jmt@ri.ac.uk (J.M. Thomas), robert@ri.ac.uk (R. Raja).

because organometallic species are rather bulky, it follows that when they are anchored (tethered or grafted: these terms are used synonymously in this article) at solid surfaces their points of attachment are rather far removed from one another (never less than some 10 Å or so). This means that when the organometallic species is subsequently converted, by appropriate post-immobilization treatment, to a smaller catalytically active entity these active sites are so far apart that the resulting solid may legitimately be designated a 'single-site' catalyst. Second, an organometallic species that exhibits high catalytic activity and selectivity when in solution is even more desirable if it is immobilized because of the ensuing advantage of ease of separation of the catalyst itself from products and from unconverted reactants. This is particularly true when one is dealing with asymmetric chiral catalysts since it is feasible (as we outline below) to boost the degree of enantioselectivity of such as catalyst by adroit manipulation of the curvature of the support. Third, a multi-nuclear organometallic species, such as a mixed-metal carbonylate, once immobilized and distributed in a spatially uniform manner on the inner walls of nanoporous supports, may be gently decarbonylated and converted into well-defined, monodispersed nanoparticle bimetallic catalysts that display exceptional activity and selectivity.

Immobilization, as used in this article, refers mainly to anchoring at the siliceous nanoporous support where the sharply defined diameter of the pores may fall (controllably) within the range 30–500 Å. But it also refers to the so-called 'ship-in-bottle' constructions in which an active organometallic catalyst is either assembled within the cages of an appropriate zeolite or, alternatively, when a zeolitic cage is built around the organometallic species (giving rise to what has also been termed a 'tea-bag' catalyst).

All the above types of immobilized organometallic catalysts are of considerable academic interest, not least because of the challenges in detailed characterization that they pose, but also because they constitute admirable test beds (or model systems) for the deeper understanding of catalytic conversion. In addition, these kinds of catalyst are likely to be of profound commercial and economic significance in that they pave the way, as we show below, to the production of catalysts that should facilitate the arrival of clean technology and green chemistry. We shall cite examples where there are already clear signs that these catalysts have reached the stage of potential commercial exploitation.

2. Types of support

The term immobilization among chemists generally implies the use of any or all the following materials as supports: silica, alumina, silica–alumina (and variants thereof including sulfated alumina to render it more acidic), magnesia, titania, zirconia, ceria, vanadia and various kinds of polymers. For our purposes, the advantages in using silica are overwhelming. The merits of having readily available high-area (ca. 600–1000 $m^2 g^{-1}$) silica with well-defined pore dimensions are obviously attractive to the catalyst merchant. In addition, owing to its excellent thermal and chemical stability, ease of handling and profusion of exposed silanol groups, silica is ideal for heterogenization of molecular catalysts. Moreover silica as a support has a rather rigid structure and does not swell when immersed in solvents, so that it may conveniently be used at both high and low temperature and at high pressure, in sharp contrast to most organic supports (e.g., styrenes). Its very inflexibility and non-compressibility also make silica-tethered (anchored or grafted) catalysts suitable for use in continuous-flow reactors. This is a potentially key factor in chemical engineering situations.

With the availability since the early 1990s (thanks to the work of groups at the Mobil Co., USA [1] and at the Toyota Co. and Waseda University, Japan [2]) of readily preparable mesoporous silica (belonging to the so-called M41S and FSM families, respectively) a clear route [3], easily trodden by preparative chemists has existed for introducing an almost limitless range of large organic (and in particular bulky organometallic) moieties into the inner walls of high-area "crystalline" silica supports which are rich in pendant silanol groups (1–2 OH per 1 nm^2).

Zeolitic supports for 'ship-in-bottle' catalysts [4–6] are particularly useful for certain specific circumstances where it is important to prevent an active entity, such as a metalloporphyrin or metallophthalocyanine molecule from losing its activity (and selectivity) because of dimerization or other complicating side-reactions.

3. Previous relevant work: a summary

Though the advantages of silica and other stable, high-area solids as potential supports for immobilizing various kinds of catalysts were recognized over a century ago, it was not until the early 1970s that Ballard [7] and others began systematically to explore such a surface for organometallic immobilization. Many definitive studies involving the surface isolation (or 'dimer' isolation) of active sites based on Mo, Cr, Ti, Ta, Nb, Co and Fe were described by Iwasawa, Gates, Yermakov, Guczi, Kuroda, Asakura, Evans, Bianchini, Ugo, Basset and their collaborators [8–18], and Ichikawa [19] was an early investigator in the systematic exploration of zeolite-encapsulated mixed-metal cluster compounds.

Following the realization [20,21] that metal clusters could function as catalysts in solution, there developed

a growing interest (reviewed by [9]) in pursuing the catalytic possibilities of organometallic species anchored at surfaces. Basset and coworkers [18] have given a recent survey of the especial importance of immobilized, single-site organometallic catalysts anchored on non-porous silica. They cover, inter alia, olefin polymerization, olefin metathesis and hydrogenolysis of alkanes.

Marks et al. [21–23] have recently reviewed the work of others, and especially their own, on surface organozirconium (cationic) species anchored to acidic, dehydroxylated zirconia or alumina surfaces. These are exceptionally active polymerization and hydrogenation catalysts.

4. A resume of methods of characterization

Conventional tools, such as X-ray diffraction are of little value in pin-pointing the essential structural features of immobilized organometallic catalysts. Neither are they of value in arriving at the detailed atomic structure of the mixed-metal (bimetallic) nanoparticles. Much may be retrieved using FTIR and MASNMR (with or without cross-polarization). Basset's work [18] using NMR is particularly noteworthy as he and his coworkers have, in this way, achieved definitive determinations of the nature of single-site environments with silica-supported organometallic catalysts – see also [52,53] and Section 5. But even more is gained from the judicious deployment of X-ray absorption fine structure (XAFS) both at the near-edge (XANES) and well beyond (extended) the edge (EXAFS). The latter is particularly important in determining the immediate atomic environment of all the (non-light, i.e. low Z) elements in the immobilized organometallic, and especially in elucidating the nature of binuclear and multinuclear clusters and the manner in which they are bonded to their underlying support (silica). Wherever possible, the above-mentioned techniques should be used under in situ conditions so that the entire course (from dispersed state to the immobilized active catalyst) of anchoring may be charted as well as following changes, if any, during catalytic operation. Details of how this is best achieved, have been published elsewhere [24–26,31].

Ex situ techniques of characterization are also invaluable, especially the use of high-resolution electron microscopy in its various modes. In the technique known as high-angle-annular-dark-field imaging, which is carried out with a scanning transmission electron microscope (STEM) advantage is taken of Rutherford scattering, where the intensity of the scattered beam is proportional to Z^2, Z, being the atomic number of the scattering atom [27]. Not only does this technique readily reveal the location and spatial distribution of nano-

particle species distributed over a siliceous support {see Fig. 1(a)} it is also ideally suited for the tomographic analyses of such samples. Scanning transmission electron tomographs enable one to identify the precise morphology and distribution of nanoparticle catalysts inside a nanoporous silica support from a series of two-dimensional (projected) images recorded through a specimen tilt series of ±75° at 1° intervals [28,29] – see Fig. 1(b). We wish to emphasize that, although the location and morphology of the naked bimetallic clusters reported here are faithfully recorded using the STEM technique, the apparent dimension of the imaged nanoparticles can be misleading. This is because the diameter (spot size) of the probing electron beam governs the observed diameter of the imaged nanoparticles. In order to maximize the efficiency in the recording of the nanoparticle locations (and to minimize electron-beam damage of the specimen), it is convenient, in practice, to use an electron-beam diameter of about 0.5–1 nm, which inevitably means that nanoparticles that, in reality, are smaller than this, will always appear larger. It is known, however, from our XAFS results for example, that the true diameters of our nanoparticles
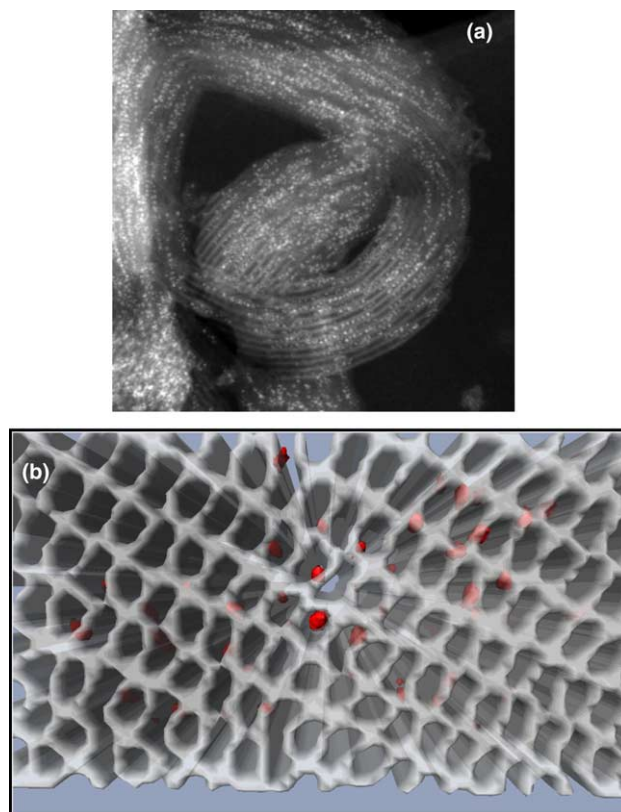

Fig. 1. Two-dimensional HAADF (High-Angle-Annular-Dark-Field) image of $Ru_{10}Pt_2$ nanoparticles anchored inside mesoporous silica (30 Å) (a), and scanning transmission electron tomograph (three-dimensional) of mesoporous silica containing $Ru_{10}Pt_2$ nanoparticle catalysts (b).

fall in the range 0.4–0.6 nm, depending upon their precise composition.

Another advantage of the STEM technique is that it readily allows the precise elemental ratio of two or more metals in a nanoparticle consisting of six or so atoms to be determined from the intensities of the respective X-ray emission peaks, stimulated by the electron beam (whose diameters may be as small as 5 Å).

5. Preparing, identifying and characterizing single-site heterogeneous catalysts derived from organometallic precursors

Preliminary studies [30] in which mesoporous silica of the MCM-41 type was synthesized from a nutrient gel into which Ti^{IV} containing alkoxide was added with a view to incorporating the transition metal in the walls of the mesoporous silica, showed that the catalytic activity of the resulting preparation in the epoxidation (using *tert*-butyl hydroperoxide, TBHP) of cyclohexene was modest (see also [30b]). When, however, Ti^{IV} active centres were grafted [31] on to the inner surfaces of mesoporous silicas using an organometallic precursor, titanocene dichloride, $Ti(Cp)_2(Cl_2)$, the catalytic performance of the resulting preparation surpassed that of the earlier preparation by a factor of ca. 10 [32]. This is because, in the second preparation, outlined in Fig. 2,

the Ti^{IV}-centred active site stands proud of the surface, not buried in it as in the earlier preparation. The detailed course of the 'heterogenization' of the Ti^{IV}-active centre was followed {from its parent $Ti(Cp)_2(Cl_2)$} by in situ XAFS combined with in situ X-ray diffractometry [33] – the former to follow the precise environment of the Ti, its valence state and its extent of coordination to neighbouring atoms, the latter to record whether the crystallinity of the mesoporous host is retained.

It is to be noted that the "half-sandwich" Ti^{IV} compound, where one of the cyclopentadienes is retained, serves as a spacer device to secure 'single-site' Ti^{IV} active centres: since the half-sandwich is an essential feature of the process of heterogenization there is no possibility for the formation of dimeric (or oligomeric) Ti^{IV} compounds as is usually the case when so-called "isolated" surface Ti centres are prepared from aqueous solutions. Our in situ EXAFS results in conjunction with our in situ FTIR measurements proves unequivocally that the catalytic site is Ti^{IV} in tetrahedral coordination, and that the Ti^{IV} ion is tripodally connected, via oxygens, to the surface of the silica. The active site is H–O–Ti–(OSi≡); there is no evidence of the occurrence of the "titanyl" group (>Ti=O) once proposed [34] as a possible structure for the active site in Ti-epoxidation catalysts.

By recording XAFS data on this Ti/SiO_2 catalyst during the course of epoxidation [35,36] the steady-state structure of the oxygen configuration around the
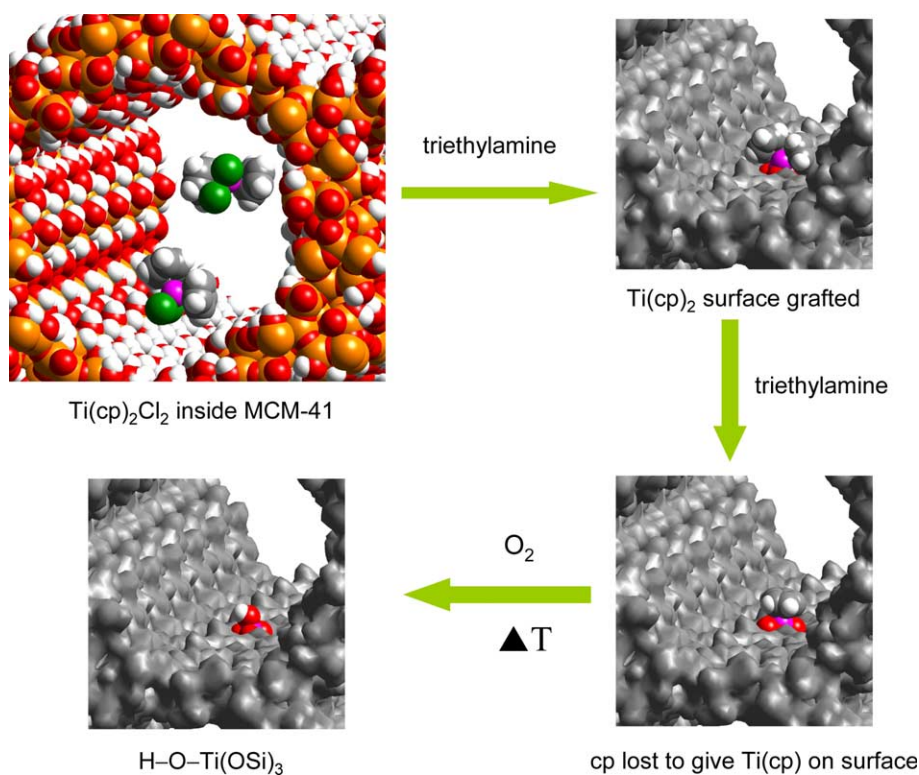

Fig. 2. The grafting of Ti^{IV}-centred active sites to the inner walls of mesoporous silica occurs via the interaction of titanocene dichloride ($Ti(Cp)_2Cl_2$) and pendant silanol groups. A half-sandwich surface compound (bottom right) forms as an intermediate (Colour code: **Ti, O, Cl,** H = white).
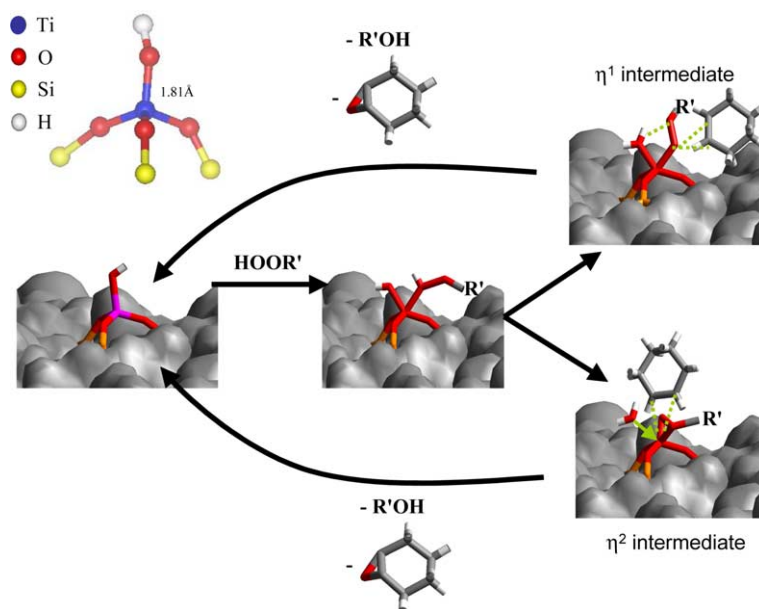
Fig. 3. Mechanism of epoxidation of cyclohexene by an alkyl hydroperoxide (HOOR′) catalyzed by the Ti[IV]-active centre tripodally bound to silica. In situ XAFS and DFT calculations indicate two plausible surface intermediates (η^1 and η^2).

Ti[IV]-active centre could be determined: it transpires that six oxygen atoms surround the Ti, at distances that could be calculated by DFT methods [36] working on plausible assumptions. This enabled a mechanism for the epoxidation of cyclohexene to be formulated (see Fig. 3) [37].

Italian workers have recently shown [38] that grafted Ti[IV]-centred catalysts (on silica) prepared by the method of [31], are very effective in epoxidizing fatty acid methyl esters (methyl oleate and methyl elaidate). They also showed that these catalysts, derived from $Ti(Cp)_2(Cl_2)$ were very effective in epoxidizing many naturally occurring terpenes [39]. The economic significance of these reports are important in that they illustrate how a number of feedstocks, hitherto derived from fossil fuel sources, for the production of industrial polymers may be obtained from plant (renewable) sources. This is a step in the appropriate direction to reach the goal of sustainable development.

Tilley et al. [40–45] have pioneered a different approach to the preparation of single-site "grafted catalysts" by using a technique that they designate a molecular precursor route. The metal ions in question cover those of Ti, Cr, Fe and vanadyl; and the essence of their preparation is that the desired atomic environment aimed at in the final catalyst (e.g., $Ti–(OSi)_4$ or $Ti–(OSi)_3$) is already present in the so-called thermolytic molecular precursor. Thus, by taking as the precursor $(^iPrO)Ti[OSi(O^tBu)_3]_3$ the environment ultimately achieved in the single-site catalyst is $(HO)–Ti–(OSi)_3$, and from the precursor $Ti[OSi(O^tBu)_3]_4$ it is $Ti–(OSi)_4$. Typical supports used by Tilley et al. were the high-area mesoporous silicas MCM-41 and SBA-15, the latter being markedly more thermally robust (because of its thicker walls). The activities of single-site 'Fe' catalysts for cyclohexene epoxidation as well as for the oxidation of benzyl alcohol to benzaldehyde were good.

There is great interest these days in the development of new catalysts for the metathesis reaction of olefins [18,46–48]. To date, and overwhelmingly, the highly active Ru(II) alkylidene catalysts which emerged from the work of Nguyen et al. [49] (typified by $L_2X_2Ru=CHR$, where X is usually Cl and L can be PPh_3 or $P(cyclohexyl)_3$) have been used homogeneously. In an enlightening article [48], Nguyen and Trnka have outlined the various methods used in assembling immobilized Ru-based olefin metathesis catalysts. The modes of attachments to a solid surface are of three kinds: (a) through the anionic ligand X, (b) through the ancillary ligands L, or (c) through the alkylidene moiety.

To date, there is only one example of the use of strategy (a); but the results are quite promising [50]. Polystyrene resin was used as the support and the actual catalyst is shown in Scheme 1.

The second strategy, attachment of the catalyst through both ancillary ligands (L), tends to reduce the catalytic activity because such a configuration hinders the loss of one ancillary ligand that is necessary for catalytic activation [51]. In the majority of cases (see Fig. 4), the Ru complex is attached to the support through the alkylidene moiety. Unfortunately, as Nguyen and Trnka point out [48], with this mode of connection the Ru complex is necessarily freed from the support after one catalytic turnover.

Coperét and coworkers [52,53], using non-porous silica supports, heat-treated to various temperatures (so as
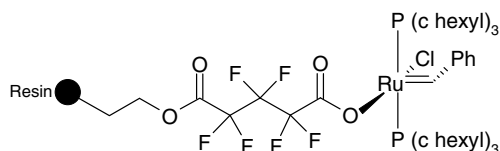
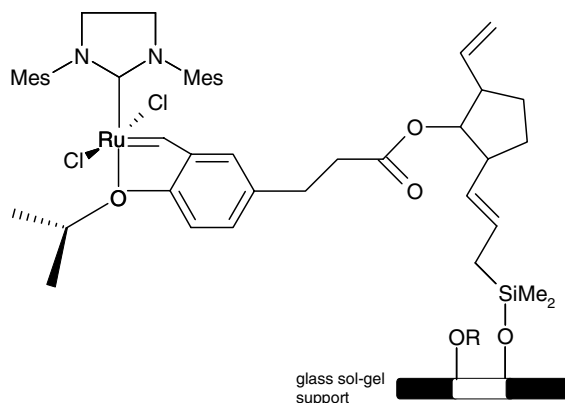Scheme 1. Ru-based olefin metathesis catalyst immobilized on polystyrene resin.

Fig. 4. Ru-based olefin metathesis catalysts immobilized on to sol–gel supports (after Nguyen et al. [48,49] and Basset et al. [17,53]).

to control the amounts of pendant silanol groups), were able to immobilize metathesis catalysts in which the central atom was either Ta, Mo, W or Re. Examples of well-defined metallocarbenes and carbynes supported on silica are shown in Fig. 5.

There are indications [53] that these immobilized catalysts exhibit activities, selectivities and lifetimes close, and in some instances superior, to those of the corresponding homogeneous catalysts.

6. A new approach to the design of chiral catalysts

Driven in part by stringent scientific and economic criteria but more specifically by ever-more demanding legislation, there is a great effort currently being mounted to discover new ways of preparing enantiomerically pure products required by the pharmaceutical and agrochemical industries as well as the contiguous fields

of flavours and fragrances. To date, the asymmetric catalysts employed both on the laboratory and industrial scale have been homogeneous. This is because such chiral catalysts possess well-defined, single-site active centres. If only because of ease of separation and recyclability, as alluded to earlier, it would be a significant step forward if single-site homogeneous (asymmetric) catalysts could be satisfactorily heterogenized. The cost alone of the rather arcane chiral ligands in current use often exceeds that of the noble metals to which they are ligated. Catalyst recovery is therefore of paramount importance for the application of enantioselective metal-centred catalysts to large-scale processes, especially in continuous-flow reactors [54].

Hitherto, almost all attempts to heterogenize homogeneous chiral catalysts have led to poor performance, principally because a spectrum [55] of different kinds of active sites were generated by the mere act of heterogenization.

The large-diameter channels of mesoporous silica – see Fig. 1(b) above – prompted us to graft sizeable chiral metal complexes and organometallic moieties on to the inner walls of these high-area solids by a variety of means that included functionalizing pendant silanol groups with alkyl halides, amines, carboxylates and phosphanes. This enabled us to prepare novel catalysts consisting of quite large (surface) concentrations of accessible, well-spaced, and structurally well-defined active sites [56]. When certain kinds of organometallic, chiral catalysts are tethered to the inner walls of a mesoporous silica it follows that the reactant's (substrate) interaction with both the pore walls and the chiral directing group will be distinct from the interaction it would experience if the chiral catalyst were free (as in the case of a homogeneous catalyst). The confinement of the reactant within the mesopore will lead to a larger influence of the chiral directing group on the orientation of the substrate relative to the reactive catalytic centre when compared to the situation in solution.

This strategic principle has been tested and its validity confirmed in several studies carried out earlier in these laboratories. See, for example, the work on allylic amination (of cinnamyl acetate and benzylamine [24,57,58]) and on the way it was exploited to boost the degree of
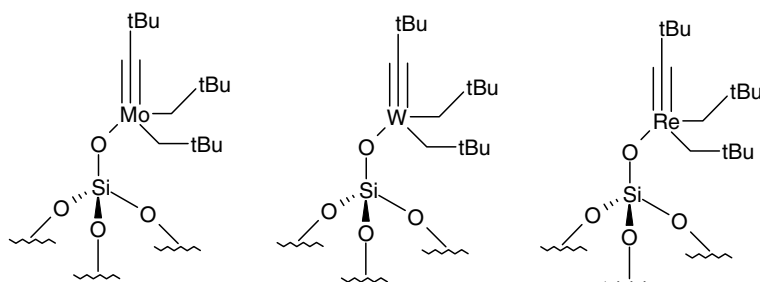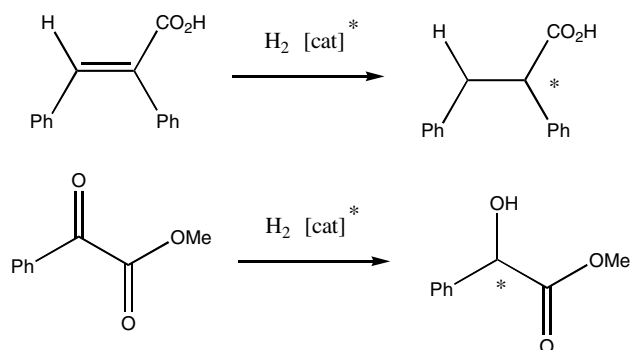

Fig. 5. Well-defined metallocarbenes and carbynes supported on silica (after Nguyen et al. [48,49] and Basset et al. [17,53]).

Scheme 2. Schematic representation of the hydrogenations of E-α-phenylcinnamic acid and methyl benzoylformate.

Fig. 6. A molecular diagram of the heterogenized single-site Rh^{I}-(S)-(−)-2-aminomethyl-1-ethyl pyrrolidine catalyst bonded to 1,5-cyclo-octadiene (COD).

enantiomeric excess of ethyl nipecotinate from ethyl nicotinate, the former being an important intermediate in biological and medicinal chemistry [59,60].

We have extended the use of the strategic principle adumbrated above in our recent work [61,62] in which, using Rh^{I} complexes with nitrogen-containing ligands – which are cheaper than phosphorus-containing ones – we investigated the following two kinds of hydrogenation, as shown in Scheme 2.

Typical chiral ligands used by us are shown in Scheme 3.

A molecular diagram of the Rh^{I} complex with AEP {(S)-(−)-2-aminomethyl-1-ethylpyrrolidine} is shown in Fig. 6. It is to be noted that the molecular cation that functions as a chiral catalyst is hydrogen-bonded to the BF$_4^-$ anion via the pendant nitrogen of the pyrrolidine.

By grafting the Rh^{I} chiral complex on both a concave silica (using MCM-41 of 30 Å diameter) and a convex silica (a non-porous silica) we established beyond doubt that the spatial restrictions imposed by the concave surface at which the active centre was located enhances the enantioselectivity of the catalyst – see Fig. 7.

Convinced of the merit (in enantioselective syntheses and other organic processes) of constraining asymmetric organometallic catalysts within siliceous nanopores (so as to increase the interaction between the pore wall and the active centre and hence to restrict access of reactant to the catalyst) we embarked on a systematic study

[63] in which a range of porous silicas was investigated. In each of these there is a very narrow spread of pore diameter. Rather than employing as porous siliceous supports the organic-template derived (MCM-41 or SBA-15) varieties, we used instead a set of commercially available desiccant silicas having narrow pore size distributions (Fig. 8) (designated Davison 923, 634 and 654). (These are made by reacting sodium silicate with a strong mineral acid (usually sulfuric acid); the pore-size being controlled by gel time, final pH, temperature, concentration of reactants, etc.). Compared to MCM-41 type silicas they are much lower in cost, more thermally and mechanically stable, less susceptible to structural collapse and available in a range of granularities. They also have some intersecting pores that facilitate the diffusion of the reactant species to the immobilized catalyst. The average diameters [64] of the pores of these silicas is, respectively, 38, 60 and 250 Å, and their respective surface areas are 700, 500 and 300 m^2 g^{-1}.

Instead of grafting the cationic Rh^{I} complex, containing the chiral diamino ligand (and cyclooctadiene, COD), using our customary covalent procedure

(S)-(-)-2-aminomethyl-1-ethylpyrrolidine (AEP)

(1R,2R)-(+)-1,2-diphenylethylenediamine (DED)

(S)-(+)-1-(2-Pyrrolidinylmethyl)-Pyrrolidine (PMP)
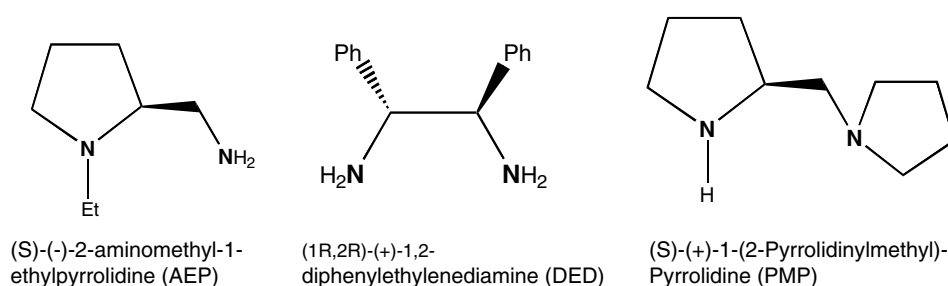
Scheme 3. Chiral ligands employed for the hydrogenations illustrated in Scheme 2.
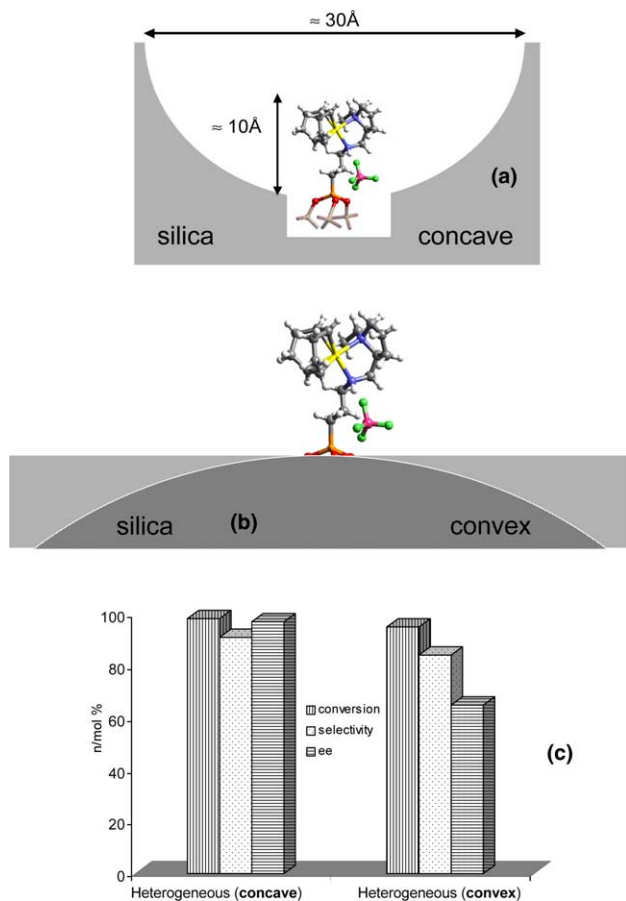
Fig. 7. Graphical model (to scale) showing the constraint at the catalyst (see Fig. 6) when anchored on a concave silica (a) in contrast to the situation on a convex (Cabosil) surface (b). The chiral diamine organometallic catalyst constrained at a concave silica surface surpasses the performance (selectivity and ee) of the same catalyst attached to a convex, non-porous silica (c).
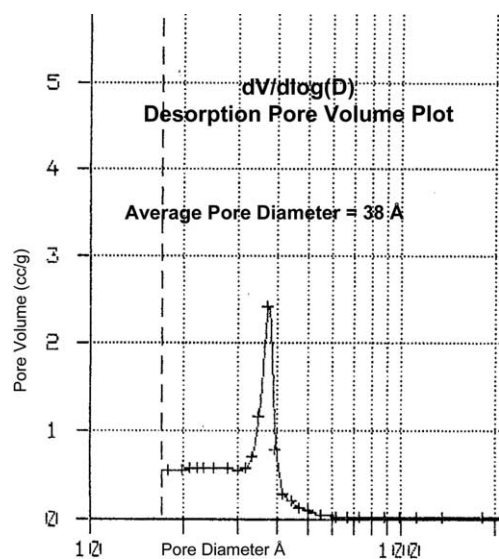
Fig. 8. Pore-size distribution curve for the mesoporous sample (Davison 923), which has a value of 38 Å, mean pore diameter [63].

(involving 3-bromopropyl-trichlorosilane to link up with a surface silanol group), we have instead employed the non-covalent immobilization approach recently described by Rege et al. [65] (see also the relevant work of Bianchini et al [66]). In this method, a surface-bound triflate $(CF_3SO_3^-)$ counter-ion securely anchors the cationic Rh(I)(COD) (Fig. 9) or the Pd(allyl) diamino complex to the inner wall. (This straightforward method circumvents the need for ligand modification to secure covalent tethering and its advantages are described fully elsewhere [62].)

The constrained chiral catalysts were:

$[Rh(COD) (S)-(-)-2\text{-Aminomethyl-1-ethyl-pyrrolidine}]^+$ $CF_3SO_3^-$ and $[Rh(COD) (S)-(+)-1\text{-2-Pyrrolidinylmethyl})\text{-pyrrolidine}]^+$ $CF_3SO_3^-$, which we abbreviate to Rh(COD)AEP and Rh(COD)PMP, respectively. And the test
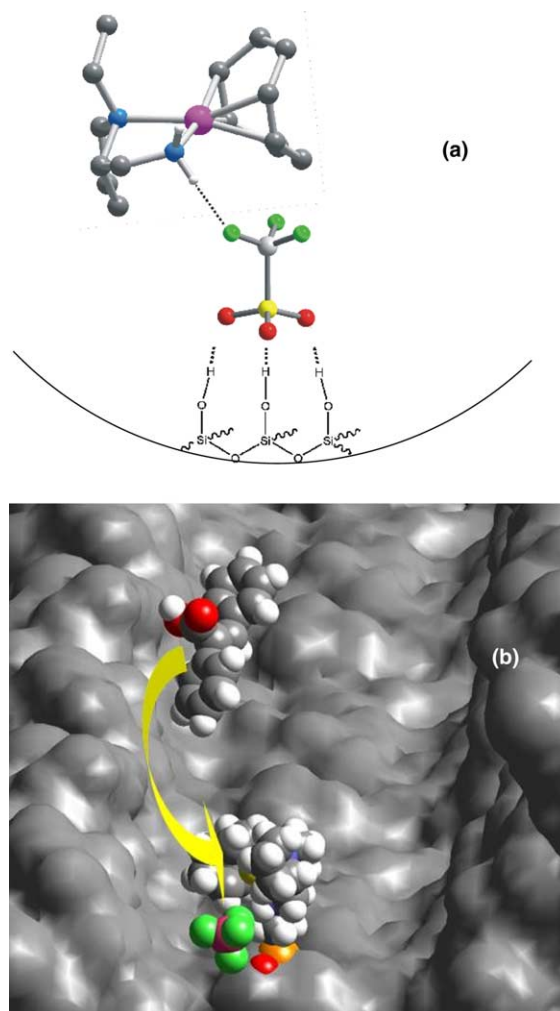
Fig. 9. (a) A triflate counter-ion, which is strongly hydrogen-bonded to the silanols of the silica, holds securely (by ionic interaction) the chiral organometallic Rh[I]-centred cation. (b) A topographic view within a concave surface showing the constraints of the catalyst once anchored onto a mesoporous surface and the spatial restrictions that dominate the approach of an incoming prochiral reactant (*E*-α-phenylcinnamic acid).

Table 1
Asymmetric hydrogenation of methyl benzoylformate

Catalyst	Type	Silica (pore dia.)	Metal	t (h)	Conv	TOF (h^{-1})	ee
Rh(COD)AEP	Homo	–	Rh(I)	2.0	62	46	0
	Het	Dav. 923	Rh(I)	0.5	82.6	542	82
		(38 Å)		2.0	93.3	153	77
		Dav. 634		0.5	67.1	440	65
		(60 Å)		2.0	93.9	154	61
		Dav. 654		0.5	44.6	292	0
		(250 Å)		2.0	86.1	141	0
Rh(COD)PMP	Homo	–	Rh(I)	0.5	46.2	145	53
	Het	Dav. 923	Rh(I)	0.5	92.8	643	85
		(38 Å)		2.0	95.8	166	94
		Dav. 634		0.5	63.0	436	72
		(60 Å)		2.0	91.5	159	78
		Dav. 654		0.5	60.7	420	65
		(250 Å)		2.0	86.9	151	59

*Reaction conditions.* Substrate ≡ 0.5 g; solvent ≡ 30 ml; H_2 ≡ 20 bar; T = 313 K; catalyst (homogeneous)≈10 mg; (heterogeneous) ≡ 50 mg; TOF = [(mol$_{substrate-converted}$)(mol$_{complex(Rh)/silica}$)$^{-1}$h^{-1}].

reaction was the asymmetric hydrogenation of methyl benzoylformate to its corresponding methyl mandelate (see Scheme 2).

In their homogeneous form, only the Rh(COD)PMP exhibits any significant enantioselectivity (ee) under the reaction conditions (see Table 1) employed by us, whereas the Rh(COD)AEP did not display any significant ee. This is probably because the bulkiness of PMP in comparison to AEP exerts further spatial congestion in the vicinity of the active centre.

Table 1 summarizes the results and shows that, as expected from arguments given above, chiral restriction does indeed boost the ee values in a manner that logically reflects the declining influence of spatial constraint in proceeding from 38 to 60 Å to the 250 Å pore-diameter silica. In the heterogeneous catalysts, the Rh(COD)PMP again, displays a higher degree of enantioselectivity when compared to the Rh(COD)AEP (due to the comparatively larger bulkiness and hence enhanced spatial congestion in the vicinity of the active centre of the PMP ligand), and it is clear that even when some of the asymmetric catalysts exhibit significant ee's under homogeneous conditions, their performance is much enhanced when immobilized in a constrained environment. It is also noteworthy that the non-covalent method of anchoring the organometallic catalyst does not lead to facile leaching when the catalyst is recycled. Further experimental details are given in patents [67] recently filed by German industry.

Although, in general, enzymes are at present more widely used industrially than asymmetric transition-metal complexes for enantioselective catalytic conversions involving pharmaceuticals and agrochemicals, the latter are of increasing importance and are more generally applicable especially for reactions that cannot be catalyzed enzymatically. In commenting on our earlier preliminary work on constrained catalysts, the authors [68] of a recent comprehensive text on the role of heterogeneous catalysts in the production of fine chemicals remarked: "*This approach seems to hold considerable promise for meeting the future challenge of developing robust, recyclable catalysts for asymmetric syntheses.*" We believe that this view is vindicated by our subsequent endeavours as evidenced in a recent Science and Technology News Feature in Chemical & Engineering News [69]. In particular, the convenience of using a non-covalently grafted chiral catalysts has obvious practical merit.

7. Functional mimics of natural enzymes (ZEOZYMES)

The ease with which nature performs many difficult chemical transformations essential to life processes has long been admired by synthetic chemists. By a judicious combination of metal ions embedded in proteinaceous supports, Nature has built an impressive array of enzymes that perform complex catalytic tasks such as reversible oxygen binding (e.g., tyrosinase), as well as selective partial oxidations of unactivated hydrocarbons (cytochrome P-450, ω-hydroxylase) and electron transport (ferridoxins). There have been intense efforts to model and mimic the catalytic function of all these enzymes – efforts driven by a desire to both understand and exploit the chemistry of their active sites.

Metalloenzymes having a metal active site owe their high selectivities in chemical reactions primarily to the protein tertiary structure, which wraps around the active site performing several crucial functions: (a) protecting the active site from deleterious reactions such as self-destruction via bimolecular pathways; (b) sieving the substrate molecules so that only those capable of passing

through the protein channels can gain access to the embedded prosthetic group, thereby enabling the enzyme high substrate- and shape-selectivity and (c) providing a stereochemically demanding void space, in the vicinity of the active site, where the substrate resides during the catalytic reaction.

The open-framework of microporous and mesoporous molecular sieves have pores, cavities and channels of molecular dimensions that select only those molecules with the proper size and shape to pass through. In general, they also orient those molecules (based on their physical dimensions) that gain access to the internal voids of the crystallite, where the active site is located. To some extent, molecular sieves have a number of striking structural similarities to the protein mantle of natural enzymes. By taking advantage of these similarities, new catalysts that combine the essential features of the robust, chemically inert molecular sieve with the high selectivity of natural enzymes may be developed. Further, fine tuning of the electronic structure, for example, by replacement of the easily oxidizable hydrogen atoms by electron-withdrawing or donating substituents in phthalocyanine or porphyrin ligands, enhances the oxidizable stability and improves the catalytic activity of these complexes. Flexibility of the ligand is responsible for these complexes to mimic the biological activity of proteins.

Metal phthalocyanine (MPc) complexes (CuPc, $CuCl_{14}Pc$, $Cu(NO_2)_4Pc$, FePc and $FeCl_{14}Pc$) were encapsulated in molecular sieves (zeolites) (see Fig. 10) by the *zeolite synthesis approach* [70,71]. Owing to their large size, metal-phthalocyanine complexes cannot be encapsulated in zeolites by anion-exchange processes. But if the zeolite is synthesized around the metal complex, then only the cage dimensions are important as far as ligand size is concerned. The zeolite synthesis method offers the further advantage of encapsulating a well-defined metal complex without contamination by uncomplexed or partially complexed metal ions as well

as by free ligands. The structural and compositional integrity of the zeolite-encapsulated-metal-phthalocyanine complexes were confirmed [72–75] using a variety of physicochemical and spectroscopic techniques (N_2 adsorption, FTIR, XRD, ESR, SEM, TGA/DTG). Computer modeling and molecular strain energy-minimization calculations [76] indicate that the geometry around the metal atom is distorted tetragonally from its square-planar symmetry when the complexes are encapsulated inside the supercages of faujasite [77]. This distortion leads to a *hydrophobic* environment around the metal atom [77b].

7.1. Methane monooxygenase (MMO) mimics

Methane monooxygenases, or MMOs, are a group of enzymes with a molecular mass of about 301 kDa, which have low-valent iron ions as the active centers that can be converted into highly reactive, high-valent iron-oxo, iron-peroxo or iron-hydroperoxo complexes. The enzymes, which are produced by certain methanotropic bacteria, catalyze the direct oxidation of methane to methanol (Scheme 4). The methanol industry generates approximately $12 billion dollars in economic revenue annually worldwide (American Methanol Institute, 2000). Currently, methanol is produced by steam reforming from natural gas in a two-step process via synthesis gas. Although significant advance has been made in conventional syngas technologies, there is no escaping the fact that it is first necessary to conduct energy-intensive endothermic steam reforming followed by subsequent catalytic conversion, which not only has thermodynamic (equilibrium) limitations, but also depletes valuable fossil fuels.

Methanol is used in the chemical industry as a building block for valuable chemicals and intermediates, as an alternative fuel source and as antifreeze. Further, MMO in methanotropic bacteria also plays a critical role in the global environment by preventing the accu-
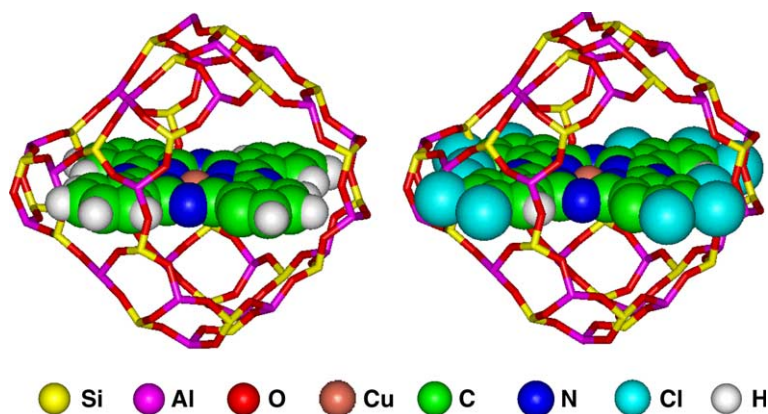

Fig. 10. Computer graphic images of copper phthalocyanine (left) and copper chlorophthalocyanine (right) encapsulated within the supercages of zeolite-X.

mulation of almost 1 billion tons of methane (a potent greenhouse gas) each year. MMO differs from other known monooxygenases in that it is able to hydroxylate stronger C–H bonds than what others are able to do, and is very versatile in oxidizing several alkanes that can be up to eight carbon atoms long, making it a strong candidate for many environmental applications since it can break down a variety of toxic chemicals and transform them into useful material. One of the major limitations in the use of this enzyme is that it is strongly inhibited and deactivated in the presence of hydrofluorocarbons and fluorinated alkanes.

The catalytic results for the oxidation of methane using air as an oxidant are summarized in Table 2. Zeolite-encapsulated phthalocyanine complexes of Fe and Cu, wherein all or most of the hydrogen atoms in the aromatic ring have been replaced with electron-withdrawing substituents such as halogens or nitro-groups, display catalytic performance that is a few orders of magnitude higher than their unsubstituted analogues. Turnover numbers in excess of 100 have been obtained with the encapsulated $FeCl_{16}Pc$ catalyst – these values are among the highest reported, so far, for the catalytic oxidation of methane at ambient conditions. A notable feature with this catalyst is the low concentration of CO_2 produced at reasonably high turnovers – this, coupled with the ease of separation, recyclability and stability of the solid catalyst make it an attractive prospect for industrial processing.

The kinetic plot (Fig. 11) shows the influence of contact time on the rate and product selectivity. A notable feature is the significant formation of both methanol and formaldehyde at lower contact times and conversions, which, plausibly, is either due to the faster rate of oxidation of methanol to formaldehyde or the simultaneous production of methanol and formaldehyde from methane. However, detailed studies [78] on the influence of catalyst weight and metal concentrations seem to suggest that the primary product of methane oxidation is methanol, which undergoes further oxidation to formaldehyde (and formic acid). It was also interesting to note [78] that solvents played a major role in fine-tuning the product selectivity, especially the production of CO_2, which was completely suppressed in the presence of acetonitrile. The ability to modulate CO_2 selectivity levels by adroit choice of solvent is an important finding, useful in the commercial exploitation of this technology.
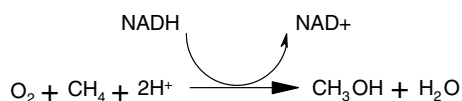
In a similar manner, propane has also been oxidized, to isopropanol using encapsulated metal-phthalocyanine complexes [79]. The direct functionalization of propane (rather than the easier alkene, propene) using air or molecular oxygen is a research challenge with significant potential in the petrochemical industry. An additional impetus for the direct oxyfunctionalization of propane is the current emphasis on the reduction of olefins and aromatics in fuels like gasoline. In view of the large worldwide resources of propane, an economic process for its direct oxidation to isopropanol is highly desirable.

7.2. Haloperoxidase mimics

Certain marine organisms have developed means to incorporate halogens into their metabolites and many of these halogenated compounds are involved in chemical defense roles. These compounds are also of pharmacological interest, due to their biological activities, which include antifungal, antiviral, antibacterial, anti-inflammatory and other actions. Haloperoxidases are enzymes which catalyze the oxidation of a halide (chloride, bromide or iodide) by hydrogen peroxide, a process that results in the concomitant halogenation of organic compounds:

$$Org - H + X^- + H_2O_2 + H^+ \rightarrow X - Org + 2H_2O$$
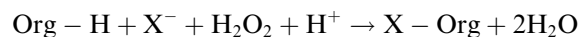
Three types of marine haloperoxidases have been identified: (1) vanadium-bromoperoxidase, a non-heme enzyme; (2) iron-heme-bromoperoxidase; and, (3) chloroperoxidases, which can utilize a chloride ion in addition to the bromide ion as donors for enzymatic halogenation reactions. Many of the spectral and magnetic properties of chloroperoxidases closely resemble those of cytochrome P-450 enzymes. In the absence of organic substrates, chloroperoxidases catalyze the peroxidation of the chloride and bromide ions to molecular chlorine and bromine respectively. These molecular

Table 2
Oxidation of methane in air

Catalyst	TON	Product selectivity (mol%)			
		CH_3OH	HCHO	HCOOH	CO_2
CuPc	0.09	–	20	–	80
$CuCl_{16}Pc$	0.72	40.2	47.5	7.2	5.1
$Cu(NO_2)_4Pc$	0.20	–	–	90	10
$FeCl_{16}$ Pc	0.90	41.2	42.0	8.3	8.5
$CuCl_{16}$ Pc–Na–X	49	51.5	41.7	4.1	2.7
$CuCl_{16}$ Pc–Na–Y	74	53.5	42.5	3.0	1.0
$Cu(NO_2)_4$ Pc–Na–X	18	–	20.5	72.0	7.5
$FeCl_{16}$ Pc–Na–X	107	52.6	42.3	3.2	1.9
$FeCl_{16}$ Pc–Na–Y	115	55.3	41.7	2.1	0.8
Na–X	–	No reaction			

Reaction conditions. Catalyst ≈ 0.75 g; $T \approx 273$ K; $t \approx 12$ h; $CH_4 \approx 50$ psig; Air ≈ 100 psig; $CH_3CN \approx 99.5$ g; TON = turnover number $\equiv [(mol_{substrate-converted})(mol_{complex(metal)})^{-1}]$.

NADH → NAD+

$$O_2 + CH_4 + 2H^+ \longrightarrow CH_3OH + H_2O$$

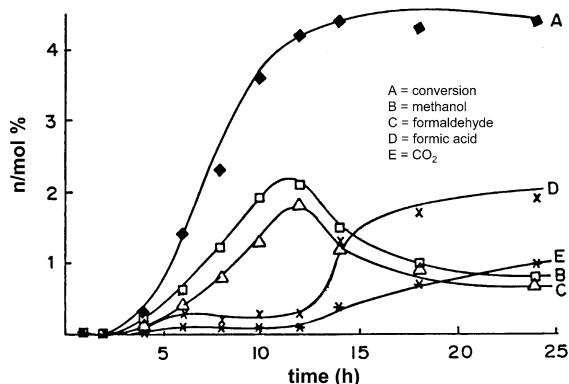Scheme 4. The methane oxidation reaction catalyzed by methane monooxygenase.

Fig. 11. Kinetic plot for the oxidation of methane using air and copper chlorophthalocyanine encapsulated in zeolite-X.

species are, however, not formed as detectable intermediates in the enzymatic halogenation of organic halogen-acceptor substrates. The rate of oxidation of a chloride or bromide to their respective molecular species is considerably slower than the rate of enzymatic chlorination or bromination of acceptor substrates.

The oxidative liberation of halogens from hydrogen halides or their salts using H_2O_2 and a suitable homogeneous catalyst is well established [80]:

$$2HX + H_2O_2 \underset{X=Cl,Br,I}{\rightarrow} X_2 + 2H_2O$$
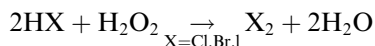
and the halogen so generated may be used for halogenating organic compounds [81]. For example, ammonium metavanadate efficiently catalyzes the oxyhalogenation of a wide variety of organic substrates in moderate yields, using H_2O_2 as oxidant, exhibiting remarkable

ortho-selectivities with electron-rich aromatics [82]. These studies [82–84] showed that *homogeneous* functional mimics of marine haloperoxidase enzymes could be successfully developed using *hydrogen peroxide* (H_2O_2) as the oxidant in combination with halide ions present in the marine environment. However, the major limitations of these processes are (1) the high cost of H_2O_2 and, (2) the recovery and disposal of the homogeneous metal catalysts, the latter posing additional environmental problems.

A solid catalyst that utilizes air or molecular oxygen as the oxidant for the oxyhalogenation of aromatic substrates at ambient conditions, using halide ions as the source of halogen, would be particularly advantageous for the following reasons: (1) in situ generation of the molecular halogen results in fuller utilization of the halogen instead of only half the available halogen; (2) easier and cheaper transport and handling of the solid alkali halides compared to molecular halogens; (3) ease of separation of recyclability of the solid catalyst; (4) air or molecular oxygen are "cheaper" and "greener" oxidants compared to H_2O_2; and, (5) avoidance of corrosive reagents (such as molecular chlorine and bromine).

The catalytic results for the oxyhalogenation of a number of industrially relevant substrates using air as an oxidant and an alkali halide are summarized in Table 3. In particular, the oxychlorination of toluene produces chlorotoluenes, which are widely used in the synthesis of chemical and pharmaceutical intermediates (for a large number of active antibiotics), as linker molecules for organic syntheses, pesticides and herbicides (agrochemicals). In general, there is the

Table 3
Oxyhalogenation of aromatics in air using $CuCl_{16}Pc$–Na–X and alkali halides

Substrate	Halide	Temp (K)	Conv (%)	Halogenated products (wt%)			
				Mono-	Di-	Tri-	Side-chain oxidation
Benzene	KCl	338	5.5	100	–	–	–
	KBr	338	6.2	100	–	–	–
Toluene	KCl	338	14.0	57.5	19.7	3.2	19.5
	KBr	338	16.8	69.5	5.5	–	25.0
Phenol	KCl	323	7.9	64.5	26.5	9.0	–
	KBr	323	18.1	62.0	25.0	13.0	–
Aniline	KCl	338	9.7	64.0	30.0	6.0	–
	KBr	338	10.3	63.0	15.5	21.5	–
Anisole	KCl	338	4.8	25.0	60.5	14.5	–
	KBr	338	6.7	25.5	55.0	19.5	–
Resorcinol	KCl	323	16.5	85.5	14.5	–	–
	KBr	323	18.2	100	–	–	–

Reaction conditions: Catalyst ≈ 0.5 g; $T \approx 338$ K; $t \approx 10$ h; Air ≈ 400 psig; Solvent (CH_3CN:H_2O) ≈ 2:1 mol%; Initiator ≈ 2 mol% TBHP (*tert*-butyl hydroperoxide).

possibility of oxyhalogenation of both the aromatic nucleus and the alkyl side-chain. Oxidation of the aromatic ring (to phenols or cresols, for example) does not occur. This is because the nucleophilic halide ions, when present, coordinate with the metal ions and suppress the formation of intermediates (like dioxygen complexes) that lead to nuclear hydroxylation. However, alkyl side-chains, are oxidized to alcohols, ketones and acids.

Mechanistic studies, including detailed kinetic and spectroscopic investigations [72], proved beyond doubt that X_2 (Br_2 or Cl_2), formed by oxidation from X^- (from K–X, where X = Br, Cl), is the halogenating agent. This augurs well with mechanistic studies using homogeneous and enzyme catalysts (see above and [80]). Further, the optimal performance of our catalyst for the oxyhalogenation reactions is in the pH range 5.5–6.0, which bears a striking resemblance to the enzyme vanadium bromoperoxidase. The use of H_2O_2 as an oxidant, instead of air, resulted in a three-fold increase in catalytic activity [72]. In summary, the observation of Br_2 during the oxyhalogenation reaction, the ortho-para orientation among the nuclear halogenated products and the pH dependence of the catalytic activity suggest that the halogenating agent is an electrophilic species and our catalyst, mimics in a restricted sense, the catalytic function of the haloperoxidase enzymes. Furthermore, the performance of these novel zeolite-encapsulated metal-complexes, as solid oxyhalogenation catalysts, in utilizing O_2 and alkyl halide ions (instead of molecular halogens) in the manufacture of halogenated aromatics has considerable promise in the organic and fine chemicals industry.
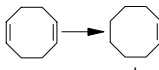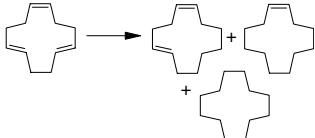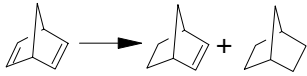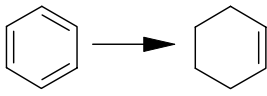
8. Monodisperse, mixed-metal nanocatalysts for selective hydrogenations

The difficulty in preparing 'monodisperse' nanoparticles of metals (or bimetals) has long been a real barrier to research into the fundamentals of heterogeneous catalysis. To use either 'incipient wetness' or 'laser ablation' methods is of little value: they each yield a wide distribution in the size of the resulting 'naked' particles. Moreover, when applied to the preparation of bimetallic nanoparticles, these methods prove inadequate.

We have found [85,86,27] that mixed-metal carbonylates (e.g. $[Ru_6Pd_6(CO)_{24}]^{2-}$), introduced into the mesopores of silica with accompanying cations such as PPN^+ [PPN≡bis-(triphenylphosphane)iminium], result in a reliable method of producing well-defined 'monodisperse' preparation of encapsulated bimetallic nanoparticles (in this case Ru_6Pd_6), the hydrogen-bonding between the pendant silanol groups (at the inner walls of the mesopores) and the –C≡O groups of the carbonylate ensuring a spatially well-distributed alignment [87] of the molecular ions within the pores. Upon subsequent gentle, thermolysis in air these aligned molecular ions are converted to quite good alignments of the naked bimetallic nanoclusters (of, for example, Ru_6Pd_6). As described elsewhere [26], this method of preparation, unlike others (e.g. involving insertion of $[PtRu_5(CO)_{16}]$ neutral entities [88]), is a reliable means of securing both monodisperse nanoparticles and retention of the element ratio of the parent carbonylate. The diameter of individual nanoparticles prepared in this way is governed primarily by the number of atoms in the final, naked cluster. Typically, a Ru_5Pt cluster is some 0.5 nm in diameter, and a $Ru_{12}Cu_4C_2$ cluster is in excess

Table 4

Single-step, highly active and selective nanoparticle catalysts for the solvent-free hydrogenation of some key organic compounds

Catalyst	Reaction	t (h)	TOF (h^{-1})	Commercial significance
Pd_6Ru_6/SiO_2		8	2012	Polymer intermediates, ketones and polyesters
Ru_6Sn/SiO_2		8	1980	
Cu_4Ru_{12}/SiO_2		8	690	
Pd_6Ru_6/SiO_2		8	5350	Laurolactam, copolyamides, nylon intermediates
Ru_6Sn/SiO_2		8	1940	
Pd_6Ru_6/SiO_2		8	11176	Coatings, lactones, polymers
Ru_6Sn/SiO_2		8	10210	
Ru_5Pt_1/SiO_2		6	2625	Starting material in production of K-A oil
$Ru_{10}Pt_2/SiO_2$		6	1790	
Pd_6Ru_6/SiO_2		6	3216	

of 1 nm. (The precise value is not easy to determine by high-resolution electron microscopy).

These nanoparticle bimetallic catalysts display very high activities in hydrogenation processes (of many kinds), and are also highly selective (see Table 4). The selectivity is often very dependent upon temperature. Because of the minuteness of the nanoparticles each atom in them is also exposed at the surface of the nanoparticle and is, therefore, coordinatively unsaturated. Turnover frequencies displayed by the Ru_6Pd_6 nanocluster in 1-hexene hydrogenation (test reaction) is a factor of ten or more in excess of those for monoelemental Pd or Ru clusters [26]. Moreover, many of these mesopore-silica-supported bimetallic nanoparticles function extremely efficiently in solvent-free hydrogenation reactions of a kind that have considerable commercial significance (see Table 4).

Insofar as the reasons for the synergy in catalytic effect between two metals in a bimetallic nanoparticle is concerned, it is not yet clear what the precise mechanism is. It is relevant to note that, with Ru_6Pd_6 nanoparticles, it is well known that Ru activates molecular hydrogen and Pd readily activates an olefinic bond. The recent work of Adams et al. [89–91] sheds more light on this general question – see, in particular, the discussion by Adams and Captain [*this volume*] of the catalytic activity in the hydrogenation of diphenylacetylene by their compound **17**, and also their recent [89] work on $[Ru_5(CO)_{15}(C)[Pt(PBu_3^t)]$. They demonstrate unequivocally (by isolating and characterizing intermediates) that Pt–Ru bonds in their (carbonylated) clusters are directly implicated in the catalytic hydrogenation of substituted acetylenes. Although our bimetallic clusters have been completely decarbonylated, it is plausible to suppose that the kind of bond scission and bond reorganization identified by Adams et al. may readily occur in our bimetallic nanoparticle catalysts.

References

[1] C.T. Kresge, M.E. Leonowicz, W.J. Roth, J.C. Vartuli, J.S. Beck, Nature 359 (1992) 710.
[2] (a) S. Inagaki, Y. Fukushima, K. Kuroda, J. Chem. Soc. Chem. Commun. (1993) 680;
(b) S. Inagaki, A. Koiwai, N. Suzuki, Y. Fukushima, K. Kuroda, Bull. Chem. Soc. Jpn. 69 (1996) 1449.
[3] J.M. Thomas, Nature 368 (1994) 289.
[4] (a) N. Herron, C.A. Tolman, J. Am. Chem. Soc. 109 (1987) 2837;
(b) D.R. Corbin, N. Herron, J. Mol. Catal. 86 (1994) 343.
[5] R. Raja, P. Ratnasamy, U.S. Patent No. US 5,767,320.
[6] A. Zsigmond, F. Notheisz, G. Csjernyik, J.E. Bäckvall, Top. Catal. 19 (2002) 119.
[7] (a) D.G.H. Ballard, Adv. Catal. 23 (1973) 263;
(b) J.P. Candlin, H. Thomas, Adv. Chem. Ser. 132 (1974) 212.
[8] Y. Iwasawa, Adv. Catal. 35 (1987) 187.
[9] (a) J. Guzman, B.C. Gates, Dalton T. (2003) 3303;
(b) B.C. Gates, in: L.L. Hegedus, A.T. Bell, N.Y. Chen, W.O. Haag, J. Wu, R. Aris, M. Boudart, G.A. Somorjai (Eds.), Catalyst Design: Progress and Perspectives, Wiley, New York, 1987, p. 71.
[10] Y.I. Yermakov, V. Zakharov, Adv. Catal. 24 (1975) 173.
[11] K. Asakura, M. Yamada, Y. Iwasawa, H. Kuroda, Chem. Lett. (1985) 511.
[12] J. Evans, S.L. Cook, G.N. Greaves, J. Chem. Soc. Chem. Commun. (1983) 1287.
[13] Y. Iwasawa, Y. Sato, H. Kuroda, J. Catal. 82 (1983) 289.
[14] (a) A. Theolier, A.K. Smith, M. Leconte, J.M. Basset, G.M. Zandergin, R. Psaro, R. Ugo, J. Organomet. Chem. 191 (1980) 1415;
(b) E. Cariati, D. Roberto, R. Ugo, E. Lucenti, Chem. Rev. 103 (2003) 3707.
[15] B.C. Gates, L. Guczi, H. Knözinger (Eds.), Metal Clusters in Catalysis, Elsevier, Amsterdam, 1986.
[16] B.F.G. Johnson, J. Lewis, P.R. Raithby, G. Süss-Fink, J. Chem. Soc. Dalton Trans. (1970) 1356.
[17] J.M. Basset, A. Choplin, J. Mol. Catal. 21 (1983) 95.
[18] C. Copéret, M. Chabanas, R.P. Saint-Arroman, J.M. Basset, Angew. Chem. Int. Ed. Engl. 42 (2003) 156, and references therein.
[19] M. Ichikawa, Adv. Catal. 38 (1992) 283.
[20] (a) E.L. Muetterties, M.J. Krause, Angew. Chem. Int. Ed. Engl. 95 (1983) 135;
(b) L. Markó, A. Vizi-Orosz, see Ref. [15], p. 170.
[21] H. Ahn, C.P. Nicholas, T.J. Marks, Organometallics 21 (2002) 178.
[22] C.P. Nicholas, H. Ahn, T.J. Marks, J. Am. Chem. Soc. 125 (2003) 1258, see also Ref. [23].
[23] T.J. Marks, J.C. Stevens (Eds.), Top. Catal. 7 (1999) 1–205 (A special issue devoted to Frontiers in Metal-Catalyzed Polymerization).
[24] J.M. Thomas, Angew. Chem. Int. Ed. Engl. 38 (1999) 3588.
[25] J.M. Thomas, G. Sankar, Acc. Chem. Res. 34 (2001) 571.
[26] J.M. Thomas, B.F.G. Johnson, R. Raja, G. Sankar, P.A. Midgley, Acc. Chem. Res. 36 (2003) 20.
[27] D. Ozkaya, W. Zhou, J.M. Thomas, V.J. Keast, P.A. Midgley, S. Hermans, Catal. Lett. 60 (1999) 101.
[28] J.M. Thomas, P.A. Midgley, Chem. Commun. (2004) 1253.
[29] P.A. Midgley, J.M. Thomas, L. Laffont, M. Weyland, R. Raja, B.F.G. Johnson, T. Khimyak, J. Phys. Chem. B. 108 (2004) 4590.
[30] (a) G. Sankar, F. Rey, J.M. Thomas, G.N. Greaves, A. Corma, B.R. Dobson, A.J. Dent, J. Chem. Soc. Chem. Commun. (1994) 2279;
(b) K. Sato, M. Aoki, R. Noyori, Science 281 (1998) 1646.
[31] T. Maschmeyer, F. Rey, G. Sankar, J.M. Thomas, Nature 378 (1995) 159.
[32] R.D. Oldroyd, J.M. Thomas, T. Maschmeyer, P.A. MacFaul, D.W. Snelgrove, K.U. Ingold, D.D.M. Wayner, Angew. Chem. Int. Ed. Engl. 35 (1996) 2787.
[33] J.W. Couves, J.M. Thomas, D. Waller, R.H. Jones, A.J. Dent, G.E. Derbyshire, G.N. Greaves, Nature 354 (1991) 465.
[34] R.A. Sheldon, J. Mol. Catal. 20 (1983) 1.
[35] J.M. Thomas, G.N. Greaves, Science 265 (1994) 1675.
[36] G. Sankar, J.M. Thomas, C.R.A. Catlow, C.M. Barker, D. Gleeson, N. Kaltsoyannis, J. Phys. Chem. B. 105 (2001) 9028.
[37] J.M. Thomas, C.R.A. Catlow, G. Sankar, Chem. Commun. (2002) 2921.

[38] M. Guidotti, N. Ravasio, P. Psaro, S. Coluccia, L. Marchese, E. Gianotti, Green Chem. 5 (2003) 421.

[39] N. Ravasio, F. Zaccheria, M. Guidotti, P. Psaro, Top. Catal. 27 (2004) 157.

[40] J. Jarupatrakorn, T.D. Tilley, J. Am. Chem. Soc. 124 (2002) 8380.

[41] T.D. Tilley, J. Mol. Catal. A. 182–183 (2002) 17.

[42] K.L. Fujdala, T.D. Tilley, J. Catal. 216 (2003) 265.

[43] C. Pak, A.T. Bell, T.D. Tilley, J. Catal. 206 (2002) 49.

[44] C. Nozaki, C.G. Lugmair, A.T. Bell, T.D. Tilley, J. Am. Chem. Soc. 124 (2002) 13194.

[45] K.L. Fujdala, T.D. Tilley, J. Catal. 218 (2003) 123.

[46] R.H. Grubbs, Acc. Chem. Res. 34 (2001) 18.

[47] A.H. Hoveyda, R.R. Schrock, Chem. Eur. J. 7 (2001) 945.

[48] S.T. Nguyen, T.M. Trnka, in: R.H. Grubbs (Ed.), Handbook of Metathesis, vol. 1, Wiley-VCH, Weinheim, 2003, p. 61.

[49] S.T. Nguyen, L.K. Johnson, R.H. Grubbs, J.W. Ziller, J. Am. Chem. Soc. 114 (1992) 3974.

[50] P. Nieczypor, W. Buchowicz, W.J.N. Meester, F.P.J.T. Rutjes, J.C. Mol, Tetrahedron Lett. 42 (2001) 7103.

[51] M.S. Sanford, J.A. Love, Ref. [48], p. 112.

[52] C. Copéret, F. Lefebvre, J.M. Basset, Ref. [48], p. 190.

[53] L. Lefort, M. Chabanas, O. Maury, D. Meunier, C. Copéret, J. Thivolle-Cazat, J.M. Basset, J. Organomet. Chem. 594 (2000) 96.

[54] C. Bianchini, P. Barbaro, Top. Catal. 19 (2002) 17.

[55] H. Brunner, in: B. Cornils, W.A. Herrmann (Eds.), Applied Homogeneous Catalysis with Organometallic Compounds, vol. 1, Wiley-VCH, Weinheim, 1996, p. 206.

[56] J.M. Thomas, T. Maschmeyer, B.F.G. Johnson, D.S. Shephard, J. Mol. Catal. A. 141 (1999) 139.

[57] B.F.G. Johnson, S.A. Raynor, D.S. Shephard, T. Maschmeyer, J.M. Thomas, G. Sankar, S.T. Bromley, R.D. Oldroyd, L. Gladden, M.D. Mantle, J. Chem. Soc. Chem. Commun. (1999) 1167.

[58] J.M. Thomas, Faraday Discuss. 100 (1995) C9.

[59] S.A. Raynor, J.M. Thomas, R. Raja, B.F.G. Johnson, R.G. Bell, M.D. Mantle, J. Chem. Soc. Chem. Commun. (2000) 1925.

[60] R.M. Laine, G. Hum, B.J. Wood, M. Dawson, Stud. Surf. Sci. Catal. 7 (1981) 1478.

[61] M.D. Jones, R. Raja, J.M. Thomas, B.F.G. Johnson, D.W. Lewis, J. Rouzard, K.D.M. Harris, Angew. Chem. Int. Ed. Engl. 42 (2003) 4326.

[62] J. Rouzard, M.D. Jones, R. Raja, B.F.G. Johnson, J.M. Thomas, M.J. Duer, Helv. Chim. Acta. 86 (2003) 1753.

[63] (a) R. Raja, J.M. Thomas, M.D. Jones, B.F.G. Johnson, D.E.W. Vaughan, J. Am. Chem. Soc. 125 (2003) 14982;
(b) M.D. Jones, R. Raja, J.M. Thomas, B.F.G. Johnson, Top. Catal. 25 (2003) 71.

[64] These values were obtained from the dV/d log(D) plots pertaining to the desorption isotherm of N_2 on the silica.

[65] F.M. de Rege, D.K. Morita, K.C. Ott, W. Tumas, R.D. Broene, J. Chem. Soc. Chem. Commun. (2000) 1797.

[66] C. Bianchini, D.G. Burnaby, J. Evans, P. Frediani, A. Meli, W. Oberhauser, R. Psaro, L. Sordelli, F. Vizza, J. Am. Chem. Soc. 121 (1999) 5961.

[67] (a) R. Raja, J.M. Thomas, M.D. Jones, B.F.G. Johnson, Process for Reducing ketocarboxylic esters, German Patent Filing No. DE 1 030 5946 (2003);
(b) R. Raja, J.M. Thomas, M.D. Jones, B.F.G. Johnson, Process for Preparing Enantiomerically Enriched α–β-hydroxycarboxylic esters, German Patent Filing No. DE 1 030 5943 (2003).

[68] R.A. Sheldon, H. van Bekkum (Eds.), Fine Chemicals Through Heterogeneous Catalysis, Wiley-VCH, Weinheim, 2001.

[69] C & EN, Science and Technology, vol. 82, March 15 2004, p. 37.

[70] R. Raja, P. Ratnasamy, European Patent No. EP 784,045 (1997).

[71] (a) R.F. Parton, I.F.J. Vankelecom, M.J.A. Casselman, C.P. Bezoukhanova, J.B. Uytterhoeven, P.A. Jacobs, Nature 370 (1994) 541;
(b) P.P. Moghe, P. Ratnasamy, R. Raja, A.V. Pol, M.G. Kotasthane, P.K. Bahirat, U.S. Patent No. US 5,786,519 (1998).

[72] R. Raja, P. Ratnasamy, J. Catal. 170 (1997) 244.

[73] R. Raja, P. Ratnasamy, Catal. Lett. 48 (1997) 1.

[74] R. Raja, P. Ratnasamy, Stud. Surf. Sci. Catal. 101 (1996) 181.

[75] S.S. Shevade, R. Raja, A.N. Kotasthane, Appl. Catal. A. 178 (1999) 243.

[76] N. Herron, J. Coord. Chem. 19 (1988) 25.

[77] (a) R. Raja, P. Ratnasamy, Stud. Surf. Sci. Catal. 103 (1997) 1037;
(b) S. Ray, S. Vasudevan, Inorg. Chem. 42 (2003) 1711.

[78] R. Raja, P. Ratnasamy, Appl. Catal. A. 158 (1997) L7.

[79] R. Raja, C.R. Jacob, P. Ratnasamy, Catal. Today 49 (1999) 171.

[80] A. Leulier, Bull. Soc. Chim. Fr. 35 (1924) 1325.

[81] R. Johnson, K. Reeve, Spec. Chem. (1992) 32.

[82] C.U. Dinesh, R. Kumar, B. Pandey, P. Kumar, J. Chem. Soc. Chem. Commun. (1995) 611.

[83] V. Conte, F.D. Furia, S. Moro, Tetrahedron Lett. 35 (1994) 7429.

[84] R.I. de la Rosa, M.J. Clague, A. Butler, J. Am. Chem. Soc. 114 (1992) 760.

[85] D.S. Shephard, T. Maschmeyer, J.M. Thomas, B.F.G. Johnson, G. Sankar, D. Ozkaya, W. Zhou, R.D. Oldroyd, R.G. Bell, Angew. Chem. Int. Ed. Engl. 36 (1997) 2242.

[86] R. Raja, G. Sankar, S. Hermans, D.S. Shephard, S. Bromley, J.M. Thomas, B.F.G. Johnson, J. Chem. Soc. Chem. Commun. (1999) 1571.

[87] W.Z. Zhou, J.M. Thomas, D.S. Shephard, B.F.G. Johnson, D. Ozkaya, T. Maschmeyer, R.G. Bell, Q.F. Ge, Science 280 (1998) 705.

[88] M.S. Nashner, A.I. Frenkel, D.M. Somerville, C.W. Hills, J.R. Sharpley, R.G. Nuzzo, J. Am. Chem. Soc. 120 (1998) 8093.

[89] R.D. Adams, B. Captain, L. Zhu, J. Am. Chem. Soc. 126 (2004) 3042.

[90] R.D. Adams, B. Captain, J. Organomet. Chem. (current issue) (2004).

[91] R.D. Adams, T.S. Barnard, Z. Li, W. Wu, J. Yamamoto, J. Am. Chem. Soc. 116 (1994) 9103.